Eur Radiol (2007) 17: 11–21
DOI 10.1007/s00330-006-0327-x

Karl-Friedrich Kreitner
R. Peter Kunz
Sebastian Ley
Katja Oberholzer
Daniel Neeb
Klaus K. Gast
Claus-Peter Heussel
Balthasar Eberle
Eckhard Mayer
Hans-Ulrich Kauczor
Christoph Düber

Chronic thromboembolic pulmonary hypertension — assessment by magnetic resonance imaging

Received: 19 December 2005
Revised: 25 April 2006
Accepted: 2 May 2006
Published online: 13 July 2006

This article is dedicated to Manfred Thelen, MD, Professor of Radiology, our teacher in clinical radiology.
This study was supported by the Deutsche Forschungsgemeinschaft (grant FOR 474/1).

K.-F. Kreitner (✉) · R. P. Kunz · S. Ley · K. Oberholzer · D. Neeb · K. K. Gast · C.-P. Heussel · C. Düber
Department of Diagnostic and Interventional Radiology,
Johannes-Gutenberg-University,
Langenbeckstrasse 1,
D-55131 Mainz, Germany
e-mail: kreitner@radiologie.klinik.uni-mainz.de
Tel.: +49-6131-174160
Fax: +49-6131-176633

S. Ley · H.-U. Kauczor
Department of Radiology,
German Cancer Research Center,
Im Neuenheimer Feld 280,
D-69120 Heidelberg, Germany

E. Mayer
Department of Heart,
Thorax and Vascular Surgery,
Johannes-Gutenberg-University,
Langenbeckstrasse 1,
D-55131 Mainz, Germany

B. Eberle
Department of Anesthesiology,
Johannes-Gutenberg-University,
Langenbeckstrasse 1,
D-55131 Mainz, Germany

Present address:
B. Eberle
Department of Anesthesiology,
Inselspital,
CH-3010 Bern, Switzerland

C.-P. Heussel
Department of Radiology, Chest Clinic at University of Heidelberg,
Amalienstrasse 5,
D-69126 Heidelberg, Germany

Abstract Chronic thromboembolic pulmonary hypertension (CTEPH) is a severe disease that has been ignored for a long time. However, with the development of improved therapeutic modalities, cardiologists and thoracic surgeons have shown increasing interest in the diagnostic work-up of this entity. The diagnosis and management of chronic thromboembolic pulmonary hypertension require a multidisciplinary approach involving the specialties of pulmonary medicine, cardiology, radiology, anesthesiology and thoracic surgery. With this approach, pulmonary endarterectomy (PEA) can be performed with an acceptable mortality rate. This review article describes the developments in magnetic resonance (MR) imaging techniques for the diagnosis of chronic thromboembolic pulmonary hypertension. Techniques include contrast-enhanced MR angiography (ce-MRA), MR perfusion imaging, phase-contrast imaging of the great vessels, cine imaging of the heart and combined perfusion-ventilation MR imaging with hyperpolarized noble gases. It is anticipated that MR imaging will play a central role in the initial diagnosis and follow-up of patients with CTEPH.

Keywords Magnetic resonance imaging techniques · Chronic thromboembolic pulmonary hypertension

Introduction and pathophysiology

Still today, the pathophysiologic events leading to chronic thromboembolic pulmonary hypertension (CTEPH) are not completely understood. The development of CTEPH seems to be an extension of the natural history of acute pulmonary embolism. Until recently, CTEPH of sufficient severity to require surgical intervention was estimated in approximately 0.1 to 0.5% of patients surviving an acute embolic event [1–3]. However, Pengo et al. showed that the cumulative incidence of symptomatic CTEPH was 3.8 percent after 2 years in patients with an acute episode of pulmonary embolism, which is significantly higher than previously suspected [4]. In their prospective and long-term

study on 314 patients, they found that younger age, a previous pulmonary embolism, a larger perfusion defect and idiopathic pulmonary embolism at presentation remained significantly associated with an increased risk of CTEPH.

For reasons still not known, pulmonary emboli in patients with CTEPH do not resolve completely after an episode of acute thromboembolism. Instead, they follow an aberrant path of organization and recanalization leading to characteristic abnormalities such as intraluminal webs and bands, pouchlike endings of arteries, irregularities of the arterial wall and stenotic lesions [2, 3, 5]. This aberrant path of obstruction and reopening occurs in repeated cycles over many years. Some data suggest that in situ thrombosis may play a major role in the development of chronic thromboembolic pulmonary hypertension. Additionally, small-vessel hypertensive arteriopathy, similar to that seen in other forms of pulmonary hypertension, seems to develop in most CTEPH patients [3, 5]. This is supported by several observations: (1) progression of pulmonary hypertension typically occurs in the absence of recurrent pulmonary embolic events or in situ pulmonary artery thrombosis; (2) there is a poor correlation between the extent of central vessel occlusion and the degree of pulmonary hypertension: this observation suggests that a component of the increased pulmonary vascular resistance results from the unobstructed, distal vascular bed; (3) histopathology demonstrates hypertensive arteriopathic changes in the resistance vessels of lung regions both involved and uninvolved in proximal vessel-organized thromboembolic disease.

During the first years, patients with CTEPH may be asymptomatic (the "honeymoon period") before mean pulmonary arterial pressure (MPAP) and pulmonary vascular resistance (PVR) in the pulmonary arteries elevate above values of 25 mmHg or 130 dyn×s×cm^{-5}, respectively. These critical values are reached after the occlusion of approximately 60% of the total diameter of the pulmonary arterial vascular bed. The longstanding increase in MPAP over 30 mmHg results in cor pulmonale ending in right heart failure with a corresponding 5-year-survival of only 30% [2, 3, 5].

The primary treatment of CTEPH is surgical pulmonary endarterectomy (PEA), which leads to a permanent improvement of the pulmonary hemodynamics [3, 6–10]. The technical feasibility and success of surgery mainly depend on the localization of the thromboembolic material: surgical accessibility is given if the organized thrombi are not located distal to the lobar arteries or to the origin of the segmental vessels in order to develop a safe dissection plane for endarterectomy [1, 6, 10]. The combination of heart and lung transplantation is only of minor importance in the treatment of these patients. In selected cases with obliterations that are located distally to the segmental level, patients with CTEPH could be candidates for balloon angioplasty [11].

The combination of multidetector-row spiral CT (MD-CT) and selective digital pulmonary angiography (DSA) is regarded as the reference standard with respect to establishing the diagnosis, assessment of the severity of the disease and the technical operability of CTEPH patients [12, 13]. MD-CT with its high in-plane and through-plane spatial resolution has proven to display the extent of thromboembolic material fully down to the sixth order branches of pulmonary vessels [14]. In combination with the retrospective gating and use of a 16- or 64-slice MD-CT scanner, the method should allow for assessment of right heart impairment [15], but data from prospective studies with CTEPH patients are still missing. Selective DSA in combination with right heart catheterization delivers essential information on mean arterial pumonary pressure (MPAP) und pulmonary vascular resistance (PVR) [2, 3].

Magnetic resonance (MR) imaging of the chest has been developped relatively recently when compared with other body areas. However, the implementation of MR angiography, lung perfusion imaging, the introduction of hyperpolarized noble gas imaging and the assessment of right heart function seem to be promising techniques for the characterization of patients with CTEPH.

This review will describe and discuss the potential of currently available MR imaging techniques in the diagnosis and management of patients with CTEPH.

Magnetic resonance imaging

Macrocirculation

For the assessment of macrocirculation in patients with CTEPH, contrast-enhanced MR angiography (ce-MRA) is the imaging technique of choice. The basic requirement is the implementation of high-gradient-strength MR systems combined with the development of short TR 3D gradient echo (GE) sequences that allow for the acquisition of breath-hold 3D Gd-enhanced data sets [16]. Modern concepts of the use of multiple array-coil elements for signal detection are the basis for the application of parallel imaging techniques: parallel imaging uses the inherent geometry of surface coils and sensitivity maps to create k-space information from under-sampled scans. Thus, the duration of the breath-holding of the MRA sequences can be significantly reduced. Acquisition times for a coronal high resolution data set (Fig. 1) with voxel sizes between 1.3×0.6×1.4 mm^3 and 1.2×1.0×1.6 mm^3 covering the whole pulmonary vasculature range between 20 and 23 s [17, 18]. However, these figures make clear that even with the application of parallel imaging techniques, true isotropic imaging has not yet been achieved for coronal data sets, and the breath-holding periods are long with respect to the mostly dyspneic patients. This is the reason why we prefer the acquisition of two sagittal data sets, one for each lung, at our institution. This enables the acquisition of true isotropic data sets with voxel sizes ranging between 1.0×1.0×1.0 and 1.2×1.2×1.2 mm^3, requiring an acquisi-

tion time between 12 and 14 s [17]. This approach furthermore guarantees that the whole pulmonary vasculature is included in the 3D volume, and the reduced acquisition times are better tolerated by the patients (Fig. 2). Each data set is enhanced by an amount of 12–16 ml of a 0.5 molar extracellular contrast agent, followed by a saline flush of 30 ml for each data set, respectively. Due to the short acquisition times of 12–14 s, a flow rate of 4 ml/s is used to optimize the synchronization of the contrast bolus with data acquisition [19]. The amount of contrast agent can be further reduced to 8–12 ml with a flow rate of 3 ml/s by the application of a higher concentrated contrast agent, e.g., the 1 molar gadobutrol agent (Schering AG, Berlin, Germany).

There is still a limited number of studies available where the usefulness of contrast-enhanced MRA in the diagnostic work-up of CTEPH has been studied. Kreitner et al. [20] showed in their study of 34 patients that ce-MRA enabled the depiction of typical findings for CTEPH: this comprised the detection of wall-adherent thromboembolic material in the central parts of the pulmonary arteries down to the segmental level, intraluminal webs and bands, abnormal proximal-to-distal tapering and abrupt vessel cutoffs. A thorough analysis of source images and the creation of multiplanar reformations were most important for the exact assessment of the morphological findings. Maximum intensity projections on the other hand provided an overview and an impression of the arterial vascular tree that was comparable to those provided by the DSA images. Compared with selective DSA, pulmonary MR angiography depicted all patent vessel segments down to the level of segmental arteries (533/533 vessel segments). For subsegmental arteries, DSA significantly detected more patent vessel segments than MRA (733 versus 681). MRA was superior to DSA in delineating the exact central beginning of the thromboembolic material. In all cases, the most proximal site as assessed by MRA corresponded to the beginning of the dissection procedure during PEA. However, as all patients suffered from CTEPH and were candidates for surgery, there was no statement possible regarding the ability of ce-MRA in the differentiation of other causes of pulmonary hypertension. Postoperatively, ce-MRA enabled the delineation of re-opened segmental arteries and a decrease in the diameter of the central pulmonary arteries. A complete normalization of pulmonary arterial vasculature was not documented in any of the cases (Fig. 1a,d).

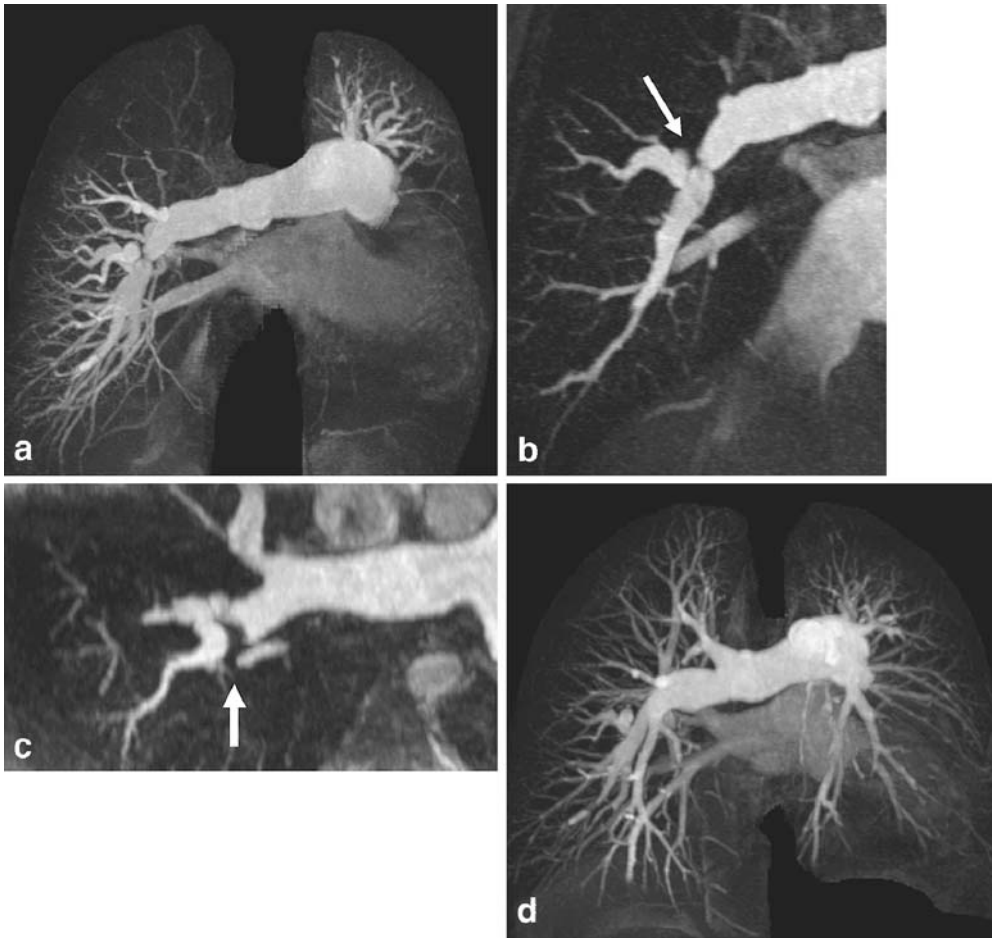

Fig. 1 Characteristic angiographic findings of a 32-year-old female CTEPH patient with intraluminal webs and bands, abrupt vessel cut-offs and abnormal proximal-to-distal tapering. **a** Maximum intensity projection (MIP) reconstruction of preoperative ce-MRA (TR/TE =3.34/1.23 ms; flip angle =25°; iPAT-factor =2; GRAPPA algorithm). **b**,**c** Multiplanar reconstructions demonstrating intralumalinal webs and bands in the pulmonary arteries (➔). **d** Postoperatively, there is a nearly complete normalization of pulmonary arterial vasculature in the right and a reopening of many segmental pulmonary arteries in the left lung

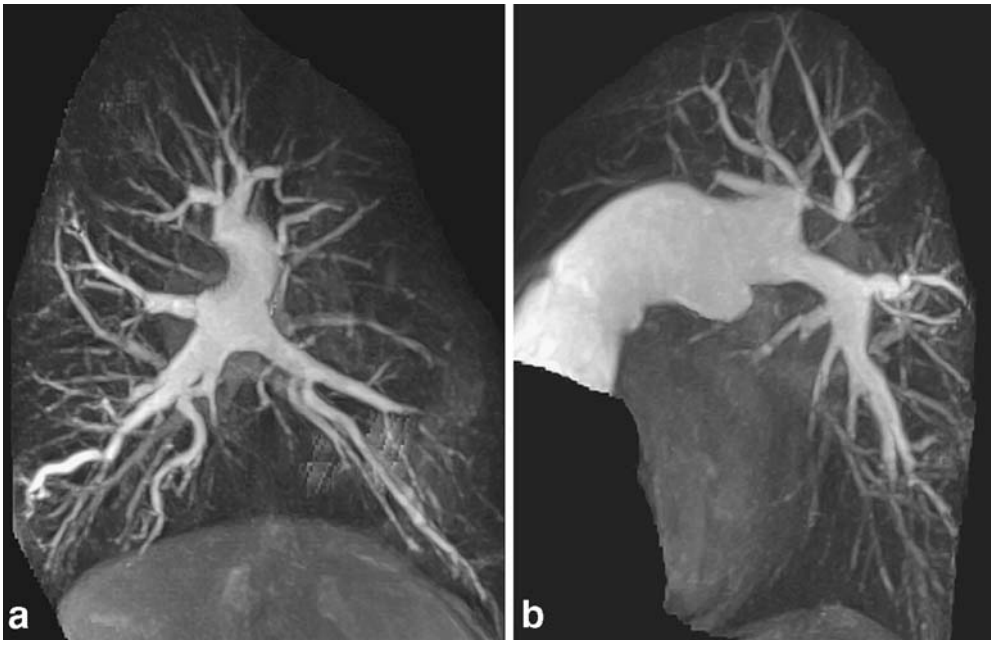

Fig. 2 **a** and **b** Sagittal data sets of right and left pulmonary arteries. MIP reconstructions of preoperative ce-MRA (TR/TE=3.34/1.24 ms; flip angle =25°; iPAT-factor =2; GRAPPA algorithm), acquisition time=13 s; 8 ml of gadobutrol. Complete coverage of the pulmonary arterial vasculature

Nikolaou and co-workers [18] in their study on 29 patients with either CTEPH or primary pulmonary hypertension (PPH) defined two categories of imaging criteria for ce-MRA: the first category focused on non-obstructing findings, e.g., dilatation of the pulmonary arterial main stem, proximal caliber changes (pruned-tree sign), peripheral vessel reduction, focal vessel ectasia and the presence of a corkscrew phenomenon. The second category comprised occluding imaging criteria such as complete vessel occlusion, free-floating thrombus, wall-adherent thromboembolic material, as well as webs and bands. The occluding criteria were considered as proof of CTEPH. Compared with DSA and/or CT-angiography, ce-MRA had sensitivities between 83 and 86% for detection of complete vessel obstructions and free-floating thrombi, and sensitivities between 50 and 71% for the depiction of older and/or organized thrombi, webs and bands. The specificities ranged between 73 and 95% for non-obstructing findings, and from 91 to 96% for occluding findings, respectively. Based on the occluding imaging criteria, the use of ce-MRA alone enabled correct differentiation of PPH and CTEPH in 24 of 29 patients (83%) in that study.

Nevertheless, in case of a good or excellent image quality, ce-MRA should identify those patients with CTEPH that delineate typical findings and that are potential candidates for surgery. Difficulties may arise in differentiating those CTEPH patients with a predominant small-vessel hypertensive arteriopathy from those with other forms of pulmonary hypertension. However, in cases with an absence of all typical angiographic findings of CTEPH, the diagnosis of primary pumonary arterial hypertension can be made (Fig. 3).

In patients with CTEPH, flow through the bronchial arteries increases because of the obstructions of the pulmonary arteries. Thus, a significant systemic to pulmonary shunt fraction is characteristic for these patients, as bronchial artery circulation in this case not only supports the lung parenchyma, but also participates in blood oxygenation. In delayed ce-MRAs of the pulmonary arteries with sufficient opacification of the thoracic aorta, those dilated bronchial arteries may be detected (Fig. 4).

Fig. 3 MIP reconstruction of a preoperative ce-MRA in a 48-year-old male who was referred to our hospital with the diagnosis of CTEPH. MR angiography revealed no characteristic findings for CTEPH so that the diagnosis was changed to primary pulmonary hypertension

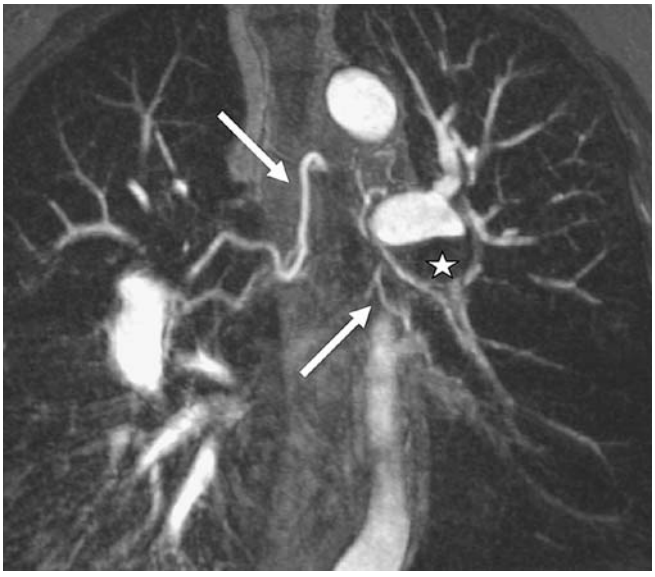

Fig. 4 Coronary MPR in a 67-year-old male patient with CTEPH. Due to a massive spread of the contrast bolus, there is a good delineation of dilated bronchial arteries (➔) supplying the parenchyma of both lungs. Note wall-adherent thromboembolic material in the left pulmonary artery (*)

They may be of additional help in distinguishing patients with CTEPH from those with primary pulmonary hypertension [21].

Microcirculation

Until recently, MR perfusion imaging has been hindered by a low SNR because of the nature of lung parenchyma, containing few protons, cardiac motion and the signal loss caused by field inhomogeneity and susceptibility artifacts at the air-tissue interfaces [22]. The desire for both qualitative and quantitative information on pulmonary microcirculation in a single study without exposure to ionizing radiation has been a strong impetus behind the investigation of MR imaging techniques for the assessment of pulmonary perfusion. The knowledge of the regional pulmonary microcirculation may become an essential parameter in patients with CTEPH: the presurgical information on the most poorly perfused lung area may influence the surgeon's strategy of PEA. Furthermore, it is of great interest to see whether the deficits in the perfusion imaging match with the findings of vessel obstruction as delineated by contrast-enhanced MRA. In this case, it informs the surgeon that the operative procedure will be successful. In those cases where perfusion deficits do not correspond to vessel obstructions, pulmonary hypertension is not maintained alone by obstructive findings of the great pulmonary arteries, and the operative procedure has a higher complication rate [3, 18].

Contrast-based perfusion MR imaging is usually performed in combination with ultra-fast 3D MRA [22, 23]. The implementation of parallel imaging techniques enabled the application of time-resolved MRA techniques that provided an angiography with reduced spatial resolution of the pulmonary arteries and perfusion-weighted data sets of the lung parenchyma. This technique allows for coverage of the whole lung volume with a temporal resolution ranging between 1.0 and 1.5 s and a voxel size ranging from 2.9×1.5×4.0 mm^3 to 3.5×1.9×4.0 mm^3 [24, 25]. Further improvements are the implementation of a view-sharing technique (TREAT) that enables either an increase in spatial or temporal resolution [26]. Recommendations for the dosage of the contrast agent vary between 0.025 and 0.1 mmol/kg body weight. Nikolaou et al. report on a linear relationship between signal increase and contrast concentration in the pulmonary artery of a healthy volunteer of up to 0.05 mmol/kg body weight. Ohno et al. found that this linear relationship changed to a non-linear one in the range between 1 and 10 mmol/l [23–25, 27]. This linear relationship is necessary for a further quantification of the resulting perfusion data instead of a semiquantitative or qualitative visual approach.

Nikolaou and co-workers studied 29 patients with pulmonary hypertension, 10 with CTEPH and 19 with primary pulmonary hypertension [18]. The basic criterion was the detection of any perfusion defect. If present, the perfusion defect was classified either as patchy and/or diffuse (indicative of PPH) or segmental and/or circumscribed (indicative of CTEPH). They used a contrast dosage of 0.1 mmol/kg body weight of the 1 molar gadobutrol that was injected with a flow of 5 ml/s. Compared with perfusion scintigraphy as the standard of reference, MR imaging had an overall sensitivity of 77% in detecting perfusion defects on a per-patient basis. Compared with the final diagnosis, MR perfusion imaging enabled a correct diagnosis of PPH or CTEPH in 20 (69%) of 29 patients. The combined interpretation of MR perfusion imaging and MR angiography led to a correct diagnosis of PPH or CTEPH in 26 (90%) of 29 patients when compared with the final reference diagnosis (combination of perfusion scinitgraphy with DSA or CT angiography).

Ley et al. in a more recent study presented preliminary results using a TREAT sequence in patients with idiopathic pulmonary arterial hypertension (IPAH) and CTEPH and compared the obtained images with those obtained from healthy volunteers [28]. They used a dose of 0.1 mmol of Gd-PTPA per kg body weight. Based on a per-segment analysis, patients with PPH showed a patchy and/or diffuse reduction of perfusion in 71 (79%) of 90 segments, a normal finding in 18 (20%) of 90 segments, and one focal defect (1%). Patients with CTEPH showed focal perfusion defects in 47 (52%), an absent segmental perfusion in 23 (26%) and a normal perfusion in 20 (22%) of 90 segments. On a per-patient basis, they had no difficulties in differentiating the two pathologic entities and in depicting the healthy volunteers. Semiquantitative analysis showed that healthy volunteers demonstrated a significantly shorter transit time than patients with IPAH and CTEPH (14±1 s

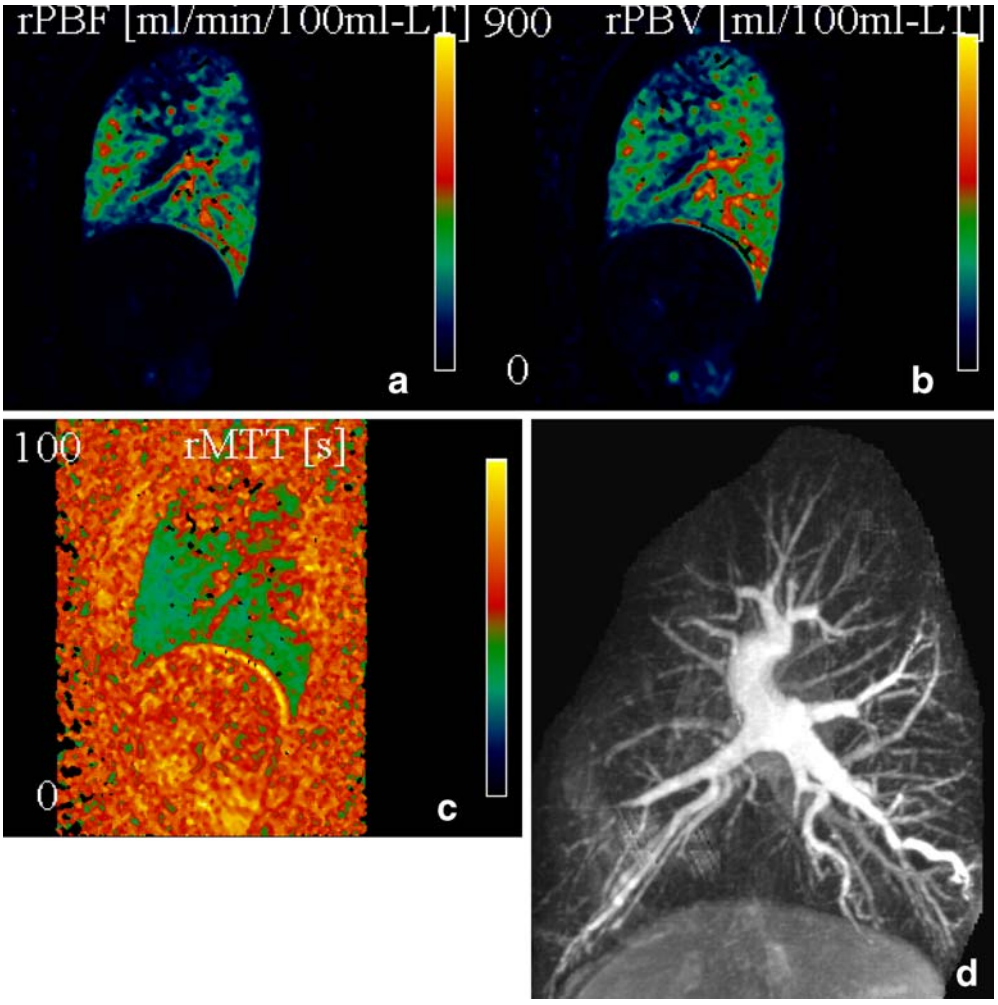

Fig. 5 Sagittal parameter maps of a quantitative perfusion data set in a 65-year-old patient with CTEPH. There are typical wedge-shaped perfusion defects in the right lung with reduced regional pulmonary blood flow (**a**), reduced regional blood volume (**b**) and increased mean transit time (MTT) (**c**). Corresponding MIP reconstruction of ce-MRA (**d**) with vessel obstruction that corresponds to the defects delineated by perfusion imaging

versus 22±4 s and 25±11 s, respectively). No difference was found between both patient populations.

In both studies [18, 27], a regional absolute quantification of lung perfusion was not done. Further studies will focus on the absolute quantification of lung perfusion where presumably lower contrast agent doses will be beneficial. First examinations in CTEPH patients revealed promising results with regard to the detection of focal perfusion defects and to the quantification of lung perfusion (Fig. 5). However, data from larger series are still missing.

Phase-contrast and cine-MR imaging

Phase-contrast measurements of flow and velocity can be regarded as a link between macro- and microcirculation. They enable the determination of cardiac output of the right and left ventricles with low inter- and intraobserver variability and can be performed selectively in the right and left pulmonary arteries [29]. Furthermore, they allow for a flow-profile analysis that could be the basis for estimation of mean pulmonary arterial pressure (MPAP) and pulmonary vascular resistance (PVR).

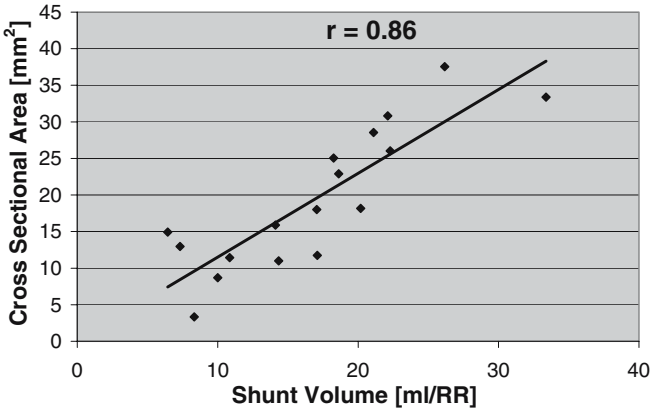

Fig. 6 Graph showing the correlation between the shunt volume, as determined by phase-contrast MR imaging, and cross-section of bronchial arteries, as determined by helical CT. Reprint with permission from [30]

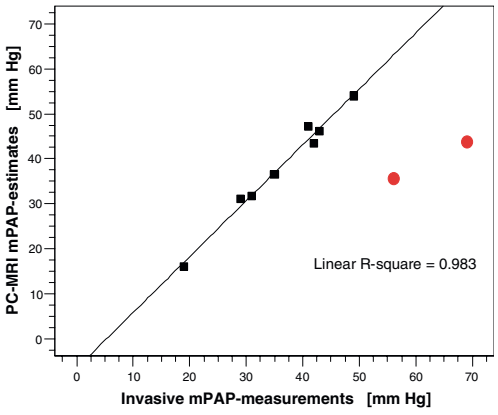

Fig. 7 Graph showing first results of the correlation between estimation of MPAP by phase-contrast MR imaging and invasively measured values

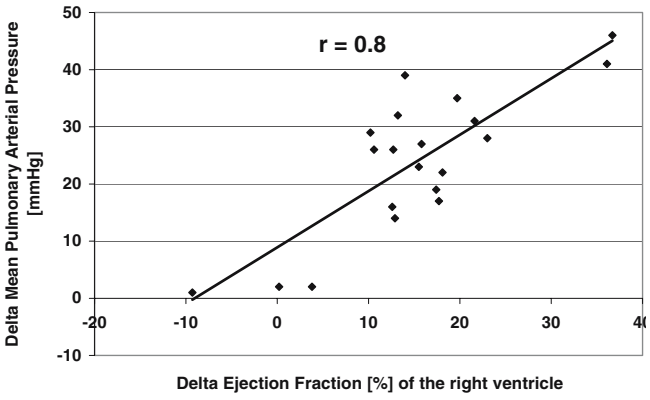

Fig. 9 Graph shows the good linear correlation between the difference of pre- and postoperative ejection fraction (delta EF) of the right ventricle and the pre- and postoperative difference in mean pulmonary arterial pressure (delta MPAP). Reprinted with permission from [20]

In the study by Kreitner et al. [20], the net forward volume in the pulmonary artery was significantly lower than that in the aorta. This flow difference can be explained by the broncho-systemic shunt volume that is caused by dilatation of bronchial arteries that originate from the aorta and supply the lung parenchyma. In a former study performed by Ley et al. [30] on a subset of CTEPH patients, there was a significant correlation between the cross-sectional area of bronchial arteries as determined by helical CT and the shunt volume between the systemic arterial and pulmonary venous circulation as determined by MR phase-contrast flow measurements (Fig. 6). After surgery, there was a complete resolution of this broncho-systemic shunt volume.

Although there was a good correlation between maximum peak velocity in the pulmonary arteries and MPAP in the study of Kreitner [20], the maximum peak velocity did not enable a reliable estimation of MPAP. This was mainly due to the limited temporal resolution of 110 ms. In the meantime, phase-contrast sequences with a temporal resolution between 10 and 12 ms were implemented for better assessment of pulmonary arterial flow [31, 32]. Based on curve parameters such as acceleration time, mean flow velocity and distensibility of the analyzed vessel, there seems to be a chance of a better assessment of MPAP. The first results are quite encouraging; however, they will have to be confirmed in larger studies before they can be recommended as a reliable tool for non-invasive assessment of MPAP by MR imaging (Fig. 7).

Cine MR imaging is an accepted reference standard for the assessment of global and regional left and right ventricular function [33, 34]. Cine imaging in CTEPH patients typically reveals a hypertrophy and dilatation of the right ventricle, a reduced right ventricular ejection fraction without substantial impairment of left ventricular

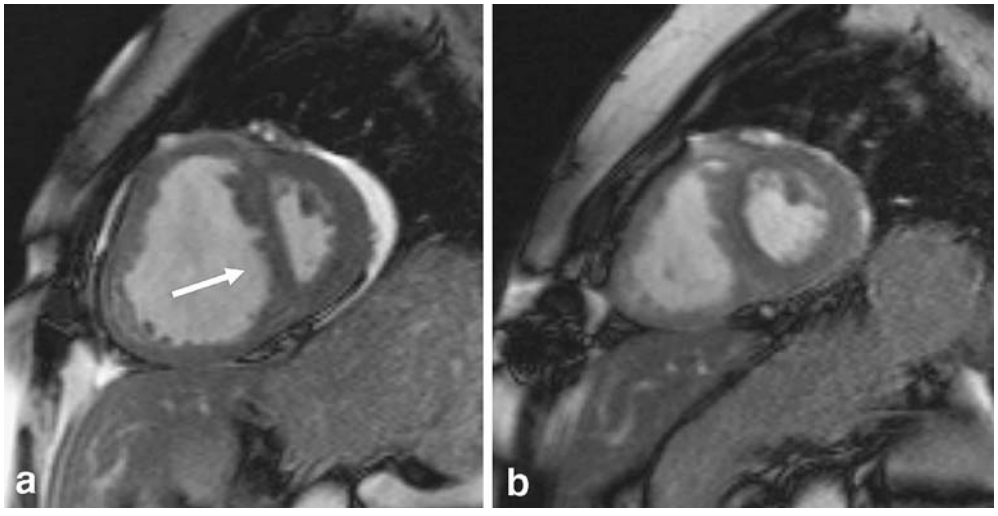

Fig. 8 Short-axis cine MR images (TE =1.27 ms; temporal resolution =34 ms) of a 73-year-old female patient showing the interventricular septum (➔) during systole. **a** Preoperative image demonstrates a paradoxical movement of the interventricular septum with bulging to the left ventricle. **b** Same patient 14 days after surgery showing a normal movement of the interventricular septum

function and a paradoxical movement of the interventricular septum. After successful PEA, there is a significant improvement or normalization of the right ventricular ejection fraction with the interventricular septum returning to a normal movement in most cases [20, 35] (Fig. 8). The increased vascular resistance in CTEPH patients goes along with a decreased ejection fraction: the right ventricular ejection fraction showed a good negative correlation with the MPAP. However, analogous to the maximum peak velocity in the same study, a precise estimation of MPAP was not possible. Interestingly, the differences between the pre- and postoperative results of the right ventricular ejection fraction and MPAP showed the best correlation (r=0.8, slope =0.98) (Fig. 9). At present, cine and phase-contrast MR imagings enable a reliable assessment of the functional improvement of the CTEPH patient after technically successful PEA [20, 35].

Functional imaging with noble gas MR imaging

Beside the low pulmonary proton density, the lungs' sponge-like structure gives rise to a large and geometrically complex gas-tissue interface, with a very inhomogeneous distribution of magnetic susceptibilities depending on the strength of B_0. This causes rapid dephasing of spin signal and, hence, a very short T2*. However, the introduction of highly spin-polarized noble gases, i.e., hyperpolarized ^{3}He and ^{129}Xe as inhaled imaging agents, has opened up a new route to achieve satisfactory spin density images of pulmonary air spaces, and even to perform functional ventilation MRI [36]. The non-equilibrium polarization ("hyperpolarization") of ^{3}He, generated by exposure to laser light, allows an increase in signal intensity in the alveolar space such that the lower density of the ^{3}He gas compared to the protons in tissue is more than overcome. This artificially strong polarization may be used to obtain superior spatial or temporal resolution.

After inhalation of the hyperpolarized ^{3}He gas, spin density images are acquired, usually in a coronal orientation for detecting ventilation defects. These images can be compared with those of MRA or perfusion imaging to see whether there are areas of preserved ventilation that demonstrate perfusion defects (mismatch). In a second step, oxygen-sensitive ^{3}He MRI is performed to determine the intrapulmonary oxygen partial pressure (PO_2) non-invasively. Molecular oxygen destroys the hyperpolarized state of the gas and thus leads to a continous signal decay. In lung regions with perfusion defects due to thromboembolic occlusions, alveolar gas exchange is reduced, leading to an increased alveolar PO_2. What initially was regarded as a drawback in ^{3}He imaging was soon found to be a possibility to measure the intrapulmonary PO_2. When taking series of images with a known interscan delay, the PO_2 can be determined by evaluation of the signal change over time in an arbitrary region of interest [37]. As the hyperpolarized state of ^{3}He is also destroyed by RF excitation, the different mechanisms of signal attenuation have to be differentiated. This is usually done by alteration of the interscan interval and the mathematical exclusion or determination of the local flip angle.

First experiments in an animal model of pulmonary embolism demonstrated the detectability of increased intrapulmonary PO_2 resulting from the obstruction of pulmonary arteries [38]. Studies with CTEPH patients showed that perfused regions demonstrated a significantly accelerated decrease of intrapulmonary oxygen partial pressure during inspiratory breath-hold when compared with non-perfused regions (Fig. 10). Furthermore, ^{3}He imaging demonstrated few regional ventilation defects that were not related to perfusion defects according to MR angiography or computed tomography. Newly developed software allows for semiautomatic oxygen mapping with high spatial resolution. Based on

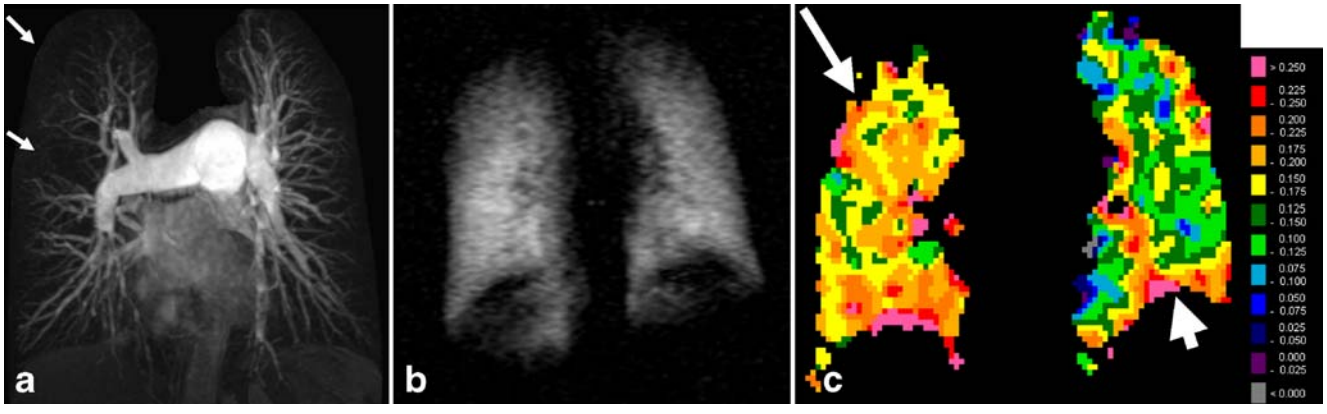

Fig. 10 A 46-year-old female suffering from CTEPH. **a** Maximum-intensity projection from a ce-MRA data set demonstrating vessel obstructions predominantly in the right upper and middle lobes (➔). **b** Ventilation image with ^{3}He: there are no apparent ventilation defects, thus together with the ce-MRA demonstrating the mismatch between macrocirculation and ventilation. **c** The O_2 parameter map shows increased intrapulmonary PO_2 in the region with disturbed perfusion (➔) when compared with areas with fewer perfusion deficits (υ)

these first results, functional ^{3}He MR imaging including techniques to utilize the oxygen-sensitivity of intraalveolar spin hyperpolarization may develop into a quick, non-invasive and easily repeatable method to assess the regional matching of ventilation with perfusion, at least in those parts of the lung reached by inhaled ^{3}He, and to estimate local oxygen uptake from selected regions within the lung parenchyma [39–41].

Perspectives and conclusions

MR imaging of the chest still today is a rapidly evolving technique whose inherent advantages of noninvasiveness, the nonionizing radiation requirement, the use of safe contrast agents and different examination techniques render it of potential value for the future. Newer developments such as direct thrombus imaging have been focused on patients with deep venous thrombosis and acute thromboembolism. For the assessment of patients with acute pulmonary embolism, the application of real-time imaging techniques using steady-state free precession sequences has shown promising results in patients with acute PE and severe dyspnea [42]. However, up to now, there are no available reports of experiences with these techniques in patients with CTEPH.

The application of contrast agents with a higher molarity or a weak protein binding to increase SNR has not shown any clear advantage over standard contrast agents if comparable dosages were used. The use of blood pool agents may be beneficial for the assessment of the pulmonary vasculature, where the short pulmonary circulation could be partially overcome with these agents. The use of an intravascular contrast agent would certainly facilitate the quantification of lung perfusion. However, after the first pass of the contrast agent, there is an enhancement of both arterial and venous structures.

Finally, in the era of upcoming 3-T machines for whole body imaging, there is still discussion with regard to the optimal field strength for the imaging of pulmonary diseases. The use of gadolinium and ^{3}He imaging could be an argument for the implementation of mid- or low-field systems with high performance gradient systems, while initial results on 3-T systems show promising results outweighing the negative effects on the field inhomogeneity at present [43].

In patients with CTEPH, currently available MR imaging techniques address various aspects of the disease: with contrast-enhanced MR angiography, the pulmonal arterial vasculature can be sufficiently analyzed down to a subsegmental level so that characteristic angiographic findings are well delineated. Furthermore, they demonstrate the proximal extent of the organized thromboembolic material with great certainty, a basic prerequisite to identify those patients that are potential candidates for pulmonary endarterectomy.

MR perfusion imaging provides information about the presence of wedge-shaped perfusion defects and whether these defects match with the findings of contrast-enhanced MRA. Thus, the knowledge of the regional pulmonary microcirculation may become an essential parameter in patients with CTEPH with respect to the presurgical information on the most poorly perfused lung area or—in case of a mismatch—pulmonary hypertension is not maintained by obstructive findings of the great pulmonary vessels alone.

Cine and phase-contrast MR imaging display the extent of the right heart impairment resulting from the underlying disease. However, one of the issues that remains to be solved is the accurate determination of pulmonary arterial blood pressure and vascular resistance; otherwise, right heart catherization will still be required [44].

Ventilation imaging with ^{3}He has made it possible to correlate perfusion and ventilation of the lung. The method also allows for mapping of the local intrapulmonary oxygen partial pressure. Thus, together with the possibilities of morphological and functional proton imaging, MR imaging certainly has the potential to play a central role in the diagnosis, differential diagnosis, treatment planning and assessment of surgical outcome in patients with CTEPH [7–9, 40].

References

1. Fedullo PF, Auger WR, Kerr KM, Rubin LJ (2001) Chronic thromboembolic pulmonary hypertension. N Engl J Med 345:1465–1472
2. Auger WR, Kerr KM, Kim NSH, Ben-Yehuda O, Knowlton KU, Fedullo PF (2004) Chronic thromboembolic pulmonary hypertension. Cardiol Clin 22:453–466
3. Darteville P, Fadel E, Mussot S, Chapelier A, Hervé P, de Perrot M, Cerrina J, Ladurie FL, Lehouerou D, Humbert M, Sitbon O, Simonneau G (2004) Chronic thromboembolic pulmonary hypertension. Eur Respir J 23:637–648
4. Pengo V, Lensing AWA, Prins MH, Marchiori A, Davidson BL, Tiozzo F, Albanese P, Biasiolo A, Pegoraro C, Iliceto S, Prandoni P (2004) Incidence of chronic thromboembolic pulmonary hypertension after pulmonary embolism. N Engl J Med 350:2257–2264
5. Frazier AA, Galvib JR, Franks TJ, Rosado-de-Christenson ML (2000) Pulmonary vasculature: hypertension and infarction. Radiographics 20:491–524
6. Dunning J, McNeil K (1999) Pulmonary thromboendarterectomy for chronic thromboembolic pulmonary hypertension. Thorax 54:755–756

7. Mayer E, Dahm M, Hake U et al (1996) Mid-term results of pulmonary hromboendarterectomy for chronic thromboembolic pulmonary hypertension. Ann Thorac Surg 61:1788–1792
8. Kramm T, Mayer E, Dahm M et al (1999) Long-term results after thromboendarterectomy for chronic pulmonary embolism. Eur J Cardiothorac Surg 15:579–583
9. Archibald CJ, Auger WR, Fedullo PF, Channick RN, Kerr KM, Jamieson SW, Kapelanski DP, Watt CN, Moser KM (1999) Long-term outcome after pulmonary thrombendarterectomy. Am J Respir Crit Care Med 160:523–528
10. Jamieson SW, Kapelanski DP (2000) Pulmonary endarterectomy. Curr Probl Surg 37:165–252
11. Feinstein JA, Goldhaber SZ, Lock JE, Ferndandes SM, Landzberg MJ (2001) Balloon pulmonary angioplasty for treatment of chronic thromboembolic pulmonary hypertension. Circulation 103:10–13
12. Schoepf UJ, Holzknecht N, Helmberger TK, Hong C, Becker CR, Reiser MF (2002) Subsegmental pulmonary emboli: improved detection with thin-collimation multi-row detector spiral CT. Radiology 222:483–490
13. Filipek MS, Gosselin MV (2004) Multidetector pulmonary CT angiography: advances in the evaluation of pulmonary arterial diseases. Semin Ultrasound CT MR 25:83–98
14. Schoepf UJ (2005) Diagnosing pulmonary embolism: time to rewrite the textbooks. Int J Cardiovasc Imaging 21:155–163
15. Koch K, Oellig F, Oberholzer K, Bender P, Kunz P, Mildenberger P, Hake U, Kreitner K-F, Thelen M (2005) Assessment of right ventricular function by 16 slice spiral-CT - comparison with magnetic resonance imaging. Eur Radiol 15:312–318
16. Kreitner K-F, Ley S, Kauczor H-U, Kalden P, Pitton MB, Mayer E, Laub G, Thelen M (2000) Die Kontrastmittelverstärkte dreidimensionale MR-Angiographie der Lungenarterien bei Patienten mit chronisch-rezidivierender Lungenembolie - Vergleich mit der selektiven intraarteriellen DSA. Fortschr Roentgenstr 172:122–128
17. Oberholzer K, Romaneehsen B, Kunz P, Kramm T, Thelen M, Kreitner K-F (2004) Kontrastmittelverstärkte 3D-MRA der Pulmonalarterien mit integrierter paralleler Akquisitionstechnik (iPAT) bei Patienten mit CTEPH - sagittale oder koronare Datenaufnahme? Fortschr Roentgenstr 176:605–609
18. Nikolaou K, Schoenberg SO, Attenberger U, Scheidler J, Dietrich O, Kuehn B, Rosa F, Huber A, Leuchte H, Baumgartner R, Behr J, Reiser MF (2005) Pulmonary arterial hypertension: diagnosis with fast perfusion MR imaging and high-spatial-resolution MR angiography - preliminary experience. Radiology 236:694–703
19. Kreitner K-F, Kunz RP, Weschler C, Ley S, Krummenauer F, Schreiber WG, Thelen M (2005) Systematische Analyse der Geometrie eines definierten Kontrastmittelbolus - Implikationen für die kontrastmittelverstärkte 3D-MR-Angiographie thorakaler Gefäße. Fortschr Roentgenstr 177:646–654
20. Kreitner K-F, Ley S, Kauczor, H-U, Mayer E, Kramm T, Pitton MB, Krummenauer F, Thelen M (2004) Chronic thromboembolic pulmonary hypertension: pre- and postoperative assessment with breath-hold magnetic resonance imaging techniques. Radiology 232:535–543
21. Remy-Jardin M, Duhamel A, Deken V, Bouaziz N, Dumont P, Remy J (2005) Systemic colateral supply in patients with chronic thromboembolic and primary pulmonary hypertension: assessment with multi-detector row helical CT angiography. Radiology 235:274–281
22. Beek EJR van, Wild JM, Fink C, Moody AR, Kauczor H-U, Oudkerk M (2003) MRI for the diagnosis of pulmonary embolism. J Magn Reson Imaging 18:627–640
23. Ohno Y, Kawamitsu H, Higashino T, Takenaka D, Watanabe H, van Cauteren M, Fujii M, Hatabu H, Sugimura K (2003) Time-resolved contrast-enhanced pulmonary MR angiography using sensitivity encoding (SENSE). J Magn Reson Imaging 17:330–336
24. Ohno Y, Hatabu H, Murase K, Higashino T, Kawamitsu H, Watanabe H, Takenaka D, Fujii M, Sugimura K (2004) Quantitative assessment of regional pulmonary perfusion in the entire lung using three-dimensional ultrafast dynamic contrast-enhanced magnetic resonance imaging: preliminary experience in 40 subjects. J Magn Reson Imaging 20:353–365
25. Fink C, Puderbach M, Bock M, Lodemann K-P, Zuna I, Schmähl A, Delorme S, Kauczor H-U (2004) Regional lung perfusion: assessment with partially parallel three-dimensional MR imaging. Radiology 231:175–184
26. Fink C, Ley S, Kroeker R, Requardt M, Kauczor H-U, Bock M (2005) Time-resolved contrast-enhanced three-dimensional magnetic resonance angiography of the chest: combination of parallel imaging with view sharing (TREAT). Invest Radiol 40:40–48
27. Nikolaou K, Schoenberg SO, Brix G, Goldman JP, Attenberger U, Kuehn B, Dietrich O, Reiser MF (2004) Quantification of pumonary blood flow and volume in healthy volunteers by dynamcic contrast-enehanced magnetic resonance imaging using a parallel imaging technique. Invest Radiol 39:537–545
28. Ley S, Fink, C, Zaporozhan J, Borst MM, Meyer FJ, Puderbach M, Eichinger M, Plathow C, Grünig E, Kreitner K-F, Kauczor H-U (2005) Value of high spatial and high temporal resolution magnetic resonance angiography for differentiation between idiopathic and thromboembolic pumonary hypertension: initial results. Eur Radiol 15:2256–2263
29. Gatehouse PD, Kewegan J, Crowe LA, Masood S, Mohiaddin RH, Kreitner K-F, Firmin DN (2005) Applications of phase-contrast flow and velocity imaging in cardiovascular MRI. Eur Radiol 15:2172–2184
30. Ley S, Kreitner K-F, Morgenstern I, Thelen M, Kauczor H-U (2002) Bronchopulmonary shunts in patients with chronic thromboembolic pulmonary hypertension. Amer J Roentgenol 179:1209–1215
31. Abolmaali ND, Seitz U, Radeloff D, Kock M, Hietschold V, Vogl TJ (2003). Assessment of pulmonary hypertension in experimental animals using high-resolution MR flow measurements. Eur Radiol 13 (Suppl 1):212–213
32. Abolmaali ND, Esmaeili A, Feist P, Ackermann H, Requardt M, Schmidt H, Vogl TJ (2004) Erstellung von Referenzwerten für die MRT-basierte Flussmessung im Truncus pulmonalis bei gesunden Kindern und Jugendlichen. Fortschr Roentgenstr 176:837–845
33. Alfakih K, Plein S, Bloomer T, Jones T, Ridgway J, Sivananthan M (2003) Comparison of right ventricular volume measurements between axial and short axis orientation using steady-state free precession magentic resonance imaging. J Magn Reson Imaging 18:25–32
34. Kunz RP, Oellig F, Krummenauer F, Oberholzer K, Romaneehsen B, Vomweg TW, Horstick G, Hayes C, Thelen M, Kreitner K-F (2005) Assessment of left ventricular function by breath-hold Cine MR imaging: comparison of different steady state free precession sequences. J Magn Reson Imaging 21:140–148

35. Ley S, Kramm T, Kauczor H-U, Mayer E, Heussel CP, Thelen M, Kreitner K-F (2003) Erfassung hämodynamischer Parameter bei Patienten mit chronisch-thromboembolischer pulmonaler Hypertonie mittels MRT vor und nach Thrombendarteriektomie. Fortschr Roentgenstr 175:1647–1654
36. Beek EJR van, Wild JM, Kauczor H-U, Schreiber W, Mugler JP, de Lange EE (2004) Functional MRI of the lung using hyperpolarized 3-Helium gas. J Magn Reson Imaging 20:540–554
37. Deninger A, Eberle B, Ebert M, Grossmann T, Heil W, Kauczor H, Lauer L, Markstaller K, Otten E, Schmiedeskamp J, Schreiber W, Surkau R, Thelen M, Weiler N (1999) Quantification of regional intrapulmonary oxygen partial pressure evaluation during apnea by 3He-MRI. J Magn Reson 141:207–216
38. Eberle B, Markstaller K, Stepniak A, Viallon M, Kauczor H-U (2002) 3Helium-MRI-Based Assessment of regional gas exchange impairment during experimental pulmonary artery occlusion. Anesthesiology 96:A1309
39. Lehmann F, Eberle B, Markstaller K, Gast KK, Schmiedeskamp J, Blümler P, Kauczor HU, Schreiber WG (2004) Ein Auswerteprogramm zur quantitativen Untersuchung der Lungenventialtion mittels dynamischer MRT von hochpolarisiertem ^{3}He. Fortschr Röntgenstr 176:1390–1398
40. Wild JM, Fichele S, Woodhouse N, Paley MNJ, Kasuboski L, Beek EJR van (2005) 3D volume-localized PO_2 measurement in the human lung with ^{3}He MRI. Magn Reson Med 53:1055–1064
41. Gast KK, Schreiber WG, Herweling A, Lehmann F, Erdös G, Schmiedeskamp J, Kauczor H-U, Eberle B (2005) Two-dimensional and three-dimensional oxygen mapping by ^{3}He-MRI validation in a lung phantom. Eur Radiol 15:1915–1922
42. Kluge A, Gerriets T, Lange U, Bachmann G (2005) MRI for short-term follow-up of acute pulmonary embolism. Assesment of thrombus appearance and pulmonary perfusion: a feasibility study. Eur Radiol 15:1969–1977
43. Pedersen MR, Fisher MT, van Beek EJR (2006) MR imaging of the pulmonary vasculature - an update. Eur Radiol DOI 10.1007/00330-005-0109-x
44. Roeleveld RJ, Marcus JT, Boonstra A, Postmus PE, Marques KM, Bronzwaqer JGF, Vonk-Nordegraf A (2005) A comparison of noninvasive MRI-based methods of estimating pulmonary artery pressure in pulmonary hypertension. J Magn Reson Imaging 22:67–72